Electronic Supplementary Material (ESI) for Nanoscale Advances.

Supplementary Information

Facile room-temperature self-assembly of extended cation-free guanine-quartet network on Mo-doped Au(111) surface

Amirreza Ghassami,[a] Elham Oleiki,[a] Dong Yeon Kim,[a] Hyung-Joon Shin,*[b] Geunsik Lee*[a] and Kwang S. Kim*[a]

[a] Center for Superfunctional Materials, Department of Chemistry, Ulsan National Institute of Science and Technology (UNIST), 50 UNIST-gil, Ulsan 44919, Republic of Korea
[b] Department of Materials Science and Engineering, Ulsan National Institute of Science and Technology (UNIST), 50 UNIST-gil, Ulsan 44919, Republic of Korea

Email: gslee@unist.ac.kr; shinhj@unist.ac.kr; kimks@unist.ac.kr

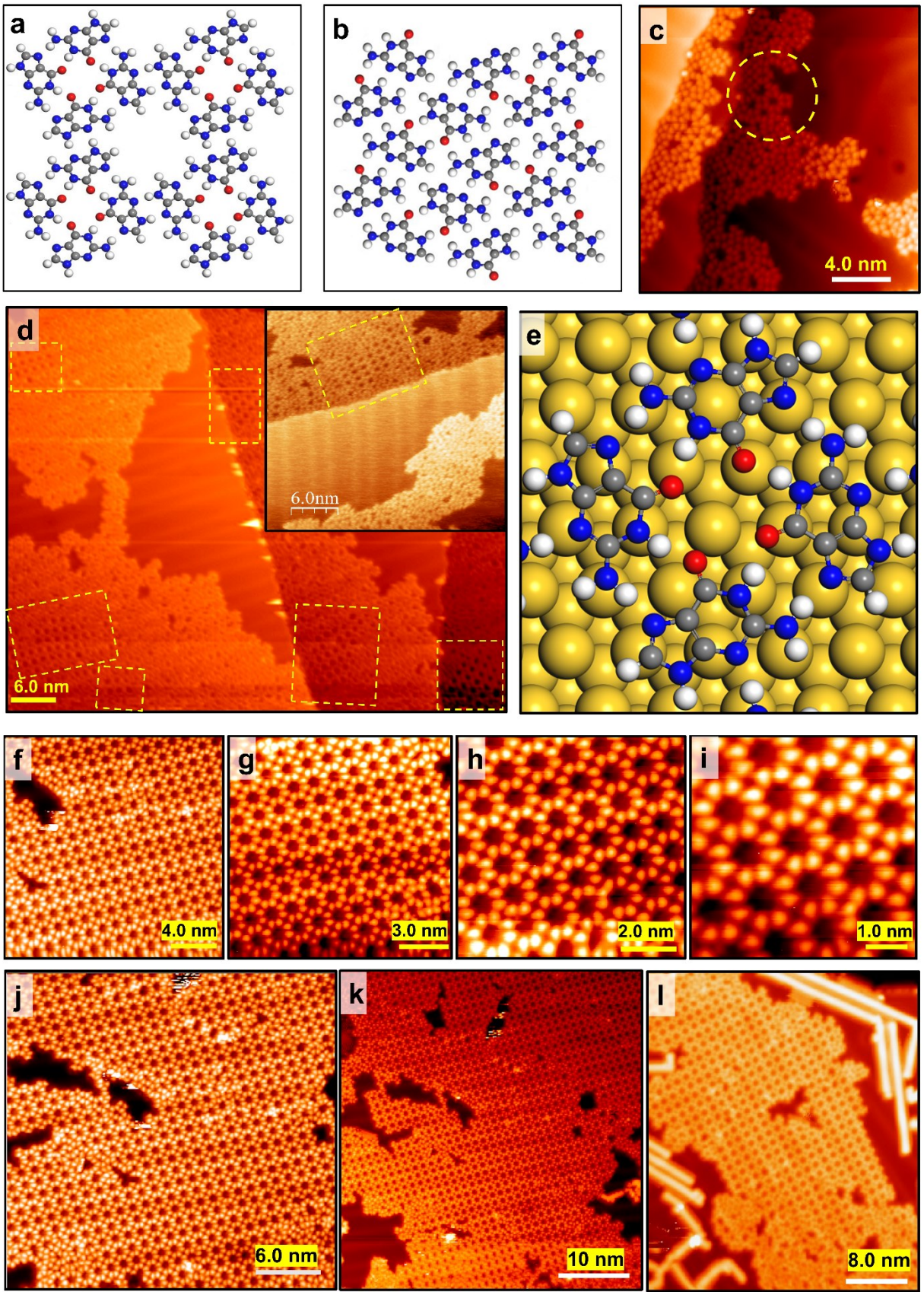
a
b
c
4.0 nm
d
6.0nm
6.0 nm
e
f
4.0 nm
g
3.0 nm
h
2.0 nm
i
1.0 nm
j
6.0 nm
k
10 nm
l
8.0 nm

Fig. S1 DFT-predicted G/9H (a) and G/7H (b) free-standing monolayers. H, white; C, gray; N, blue; O, red. (c) Initial seed of guanine-quartet network on Mo-doped Au surface without GNR pre-synthesis, which are deposited in a short time. GQ network's initial seed is shown in a yellow dashed line. (d) RT self-assembly of GQ networks coexisting with the disordered domains when Mo is embedded at the Au(111) surface. GQ networks on the Mo-doped Au surface are rare because there is a limited chance for them to grow without the interference of disordered domains coming from the step edges. The inset image shows a higher resolution of GQ network. GQ networks are highlighted in yellow dashed lines. Scanning conditions: It = 0.029 nA, Vs = +0.9 V. (e) DFT structural model of metal-free GQ network on Au(111). (f-l) GQ network on Mo-Au(111) surface with GNR pre-synthesis in various scales. Scanning conditions: I_t = 0.055 nA, V_s = +0.8 V. (j) RT assembly of GQ network coexisted with the disordered domains and is surrounded by GNRs. Scale bar: 4.0 nm in panel f, 3.0 nm in panel g, 2.0 nm in panel h, 1.0 nm in panel i. 6.0 nm in j, 10.0 nm in k, and 8.0 nm in l. GQ networks were nucleated from different seeds and grew. When they reach one another, probable networks' mismatch is inevitable. Scanning conditions in i: I_t = 0.03 nA, V_s = +1.0 V. It has been known guanine molecules quickly diffuse down to surfaces without being covered by graphene[1–3] (in our case Au(111) surface). Therefore, guanine molecules are hardly stacked on GNRs, as evidenced in our experiments, hence 7-AGNR acts as neutral fences of cage area to grow guanine SA.

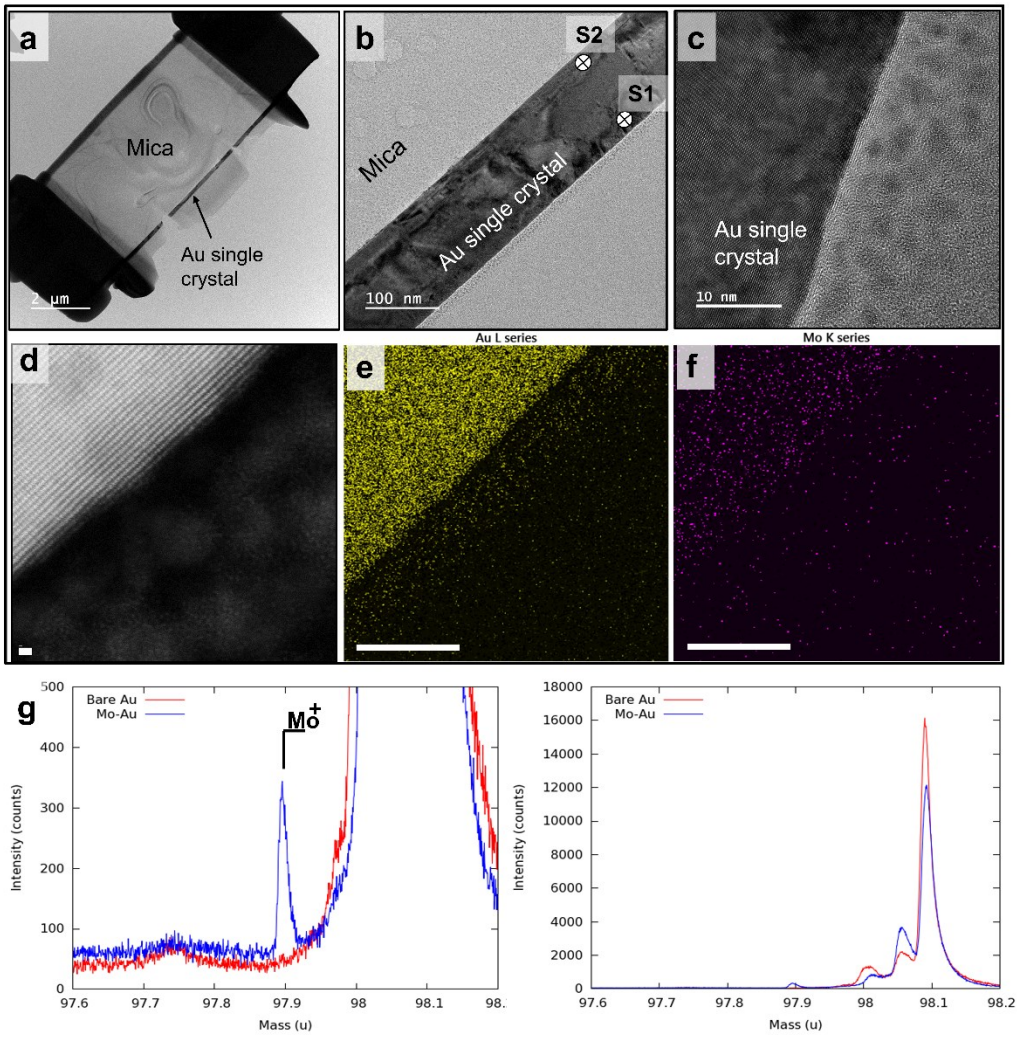

Fig. S2 (a) Electron microscopy image. (b) TEM image of Au single crystal on mica, (c) HR-TEM, and (d) HAADF-STEM of the lateral cross-section of bulk Au prepared by FIB-SEM. (e,f) The corresponding energy-dispersive X-ray spectroscopy (EDS) elemental mapping. The crystal structure of Au was unchanged after Mo was doped. Mo diffuses homogeneously over Au(111) surface. Scale bar: 2 μm in panel a, 100 nm in panel b, 10 nm in panel c, and 5.0 Å in panel d, and 25 nm in panels e and f. EDS elemental mapping shows a ~3% ratio of Mo-Au mixture **below** the Au(111) surface and a 5.5% ratio near mica at the bottom of Au(111) layers after repeatedly alloyed the Au with Mo and cleaned the surface by several cycles of annealing at 700 K [4–6] and mild Ar^+ sputtering. Therefore, the Mo concentration at the Au(111) surface layer is much less than 3%. A Mo atom substituting for an Au atom at the subsurface layer is more stable than that at the surface with **0.36 eV** of total energy difference based on DFT calculation. EDS elemental mapping also shows that Mo is more concentrated below the surface when it is annealed. To better show the Mo/Au ratio differences near the surface layer and bulk Au, peak intensities of O and C, which appear due to exposure to air, and K series of Ga, which is a residue of the FIB procedure, have been excluded. (g)

Time-of-Flight Secondary Ion Mass Spectrometry (TOF-SIMS) using a Bismuth ion beam from the Mo-Au surface also shows Mo is doped into the Au surface. The raster area is 500 × 500 μm^2.

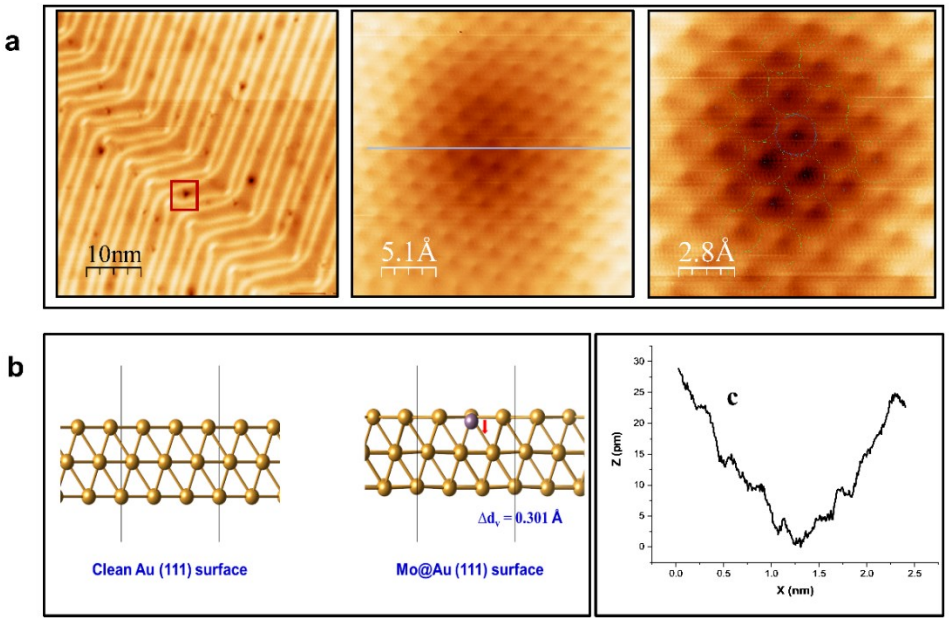

Fig. S3 Vertical Displacement (Δd$_v$) of Mo from the Au surface in the case of Mo-doped Au(111) surface. (a) STM images of Mo-induced defects at Au(111) surface after Mo were implanted in the surface. In general, the lattice structure remained unchanged. Based on TOF-SIMS and TEM-EDS, defects are induced by Mo atoms. (b) PBE calculations with cut-off energy of 500 eV. The Au/Mo-Au surfaces were built using 3x3 supercell of Au(111) surface (27 atoms). The Mo atom is buried in the Au Surface (Δd$_v$ = 0.3 Å). (c) The curve shows around 30 pm (0.3 Å) height difference, measured by STM from the middle image in (a). Scanning conditions: I_t = 0.1 nA, V_s = +0.8 V. Pristine Au(111) surface is free of defects. After Mo was implanted at the surface by first placing Mo clusters on Au surface and then annealing at 830 K; STM images showed a few defects appeared with unchanged Au(111) lattice structure. Since the Mo atom size is comparable with Au atom, distinguishing them and finding the Mo/Au ratio at the surface by STM is not accurate enough but qualitatively useful. As mentioned in Fig 5a, when the surface is covered with G/9H molecules on pristine Au surface, G/9H to G/7H transformation takes place at 400 K, but at Mo-doped Au surface, it needs 460 K for anchored G molecules to fully comply with zigzag structure. Therefore, when the implanted Mo atoms at Au surface are rare and separated from one another, the GQ network's seed initiated and grew. The optimized Mo/Au ratio is achieved when we annealed surface after Mo deposition at 830 K for 10 min and thereafter at 700 K for 30 min. With less annealing duration, clusters of Mo at Au surface remained and resulted in a lower Mo/Au ratio. More annealing duration also led to a low ratio since Mo diffuses into the Au bulk irreversibly. As shown in Fig. S7a-b, Au(111) surface is overdoped with Mo atoms by less annealing duration (830 K for 5 min), although a few separated porous structures are formed, GQ network formation is unlikely due to extra anchored molecules. 400 K annealing of this surface resulted in a similar STM image in Fig 5a.

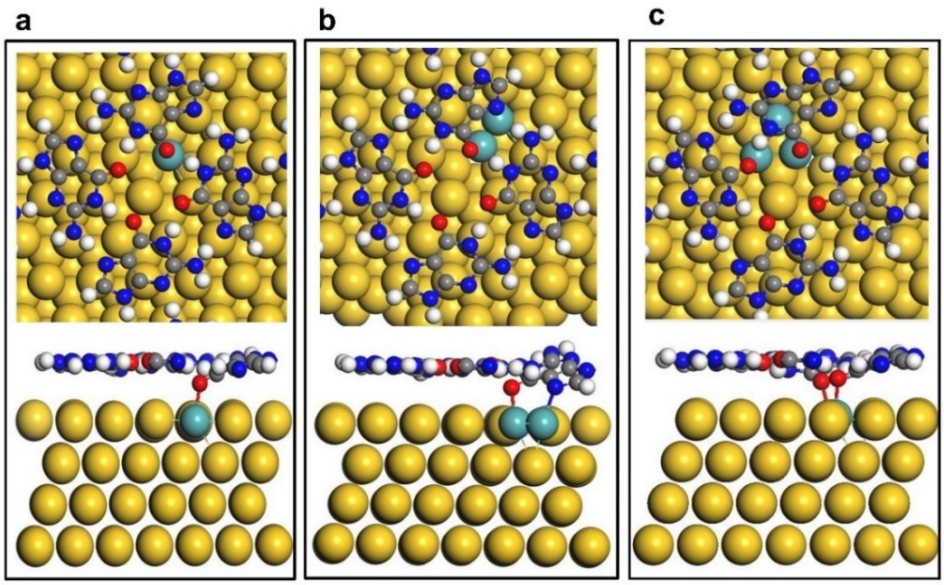

GQ network	Formation energy (eV/molecule)	Adsorption energy (eV/molecule)
Free-standing	-1.27	-
On bare Au(111) surface	-1.82	-0.55
On Mo-Au(111) surface (single Mo atom at surface)	-1.96	-0.70
On Mo-Au(111) surface (two Mo atoms at surface)	-2.17	-0.90
On Mo-Au(111) surface (three Mo atoms at surface)	-2.12	-0.85

Fig. S4 GQ adsorption on Mo-Au(111) surface. DFT-predicted geometry (side/top views) for the GQ network adsorption on the Mo-Au surface. (a) A single Mo atom is embedded at Au(111) surface. The GQ network adsorption energy is -0.70 eV. (b) Two Mo atoms are embedded at Au(111) surface. The GQ network adsorption energy is -0.90 eV. (c) Three Mo atoms are embedded at Au(111) surface. The GQ network adsorption energy is -0.85 eV. H, white; C, gray; N, blue; O, red; Mo, azure; Au, yellow. GQ network formation energies: free-standing, on pristine Au(111), and on Mo-doped Au(111) surface with one, two, or three Mo atoms embedded at the surface layer. Free standing lattice formation energy per molecule: $E_f = [E_{2D\ lattice} - 4\times E_{molecule}]/4$; lattice formation energy on the surface per molecule: $E_f = [E_{2D\ lattice@surface} - 4\times E_{molecule} - E_{surface}]/4$.

a

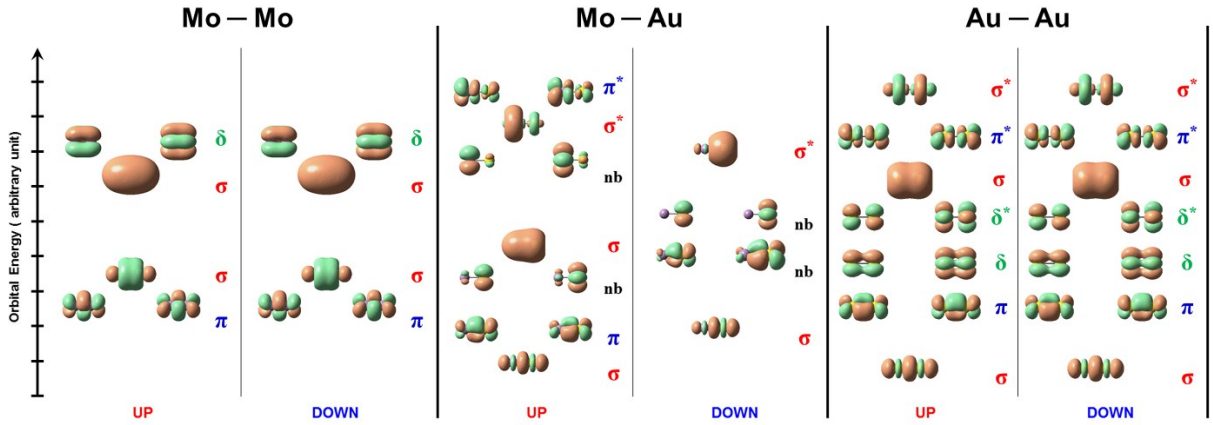

	Binding Energy (E_b)	Optimized Bond Length	Wiberg bond index (WBI)
Mo–Mo (*S*=1)	3.89 eV	1.926 Å	6.04
Mo–Au (*S*=6)	2.26 eV	2.551 Å	1.04
Au–Au (*S*=1)	2.24 eV	2.530 Å	1.03

b

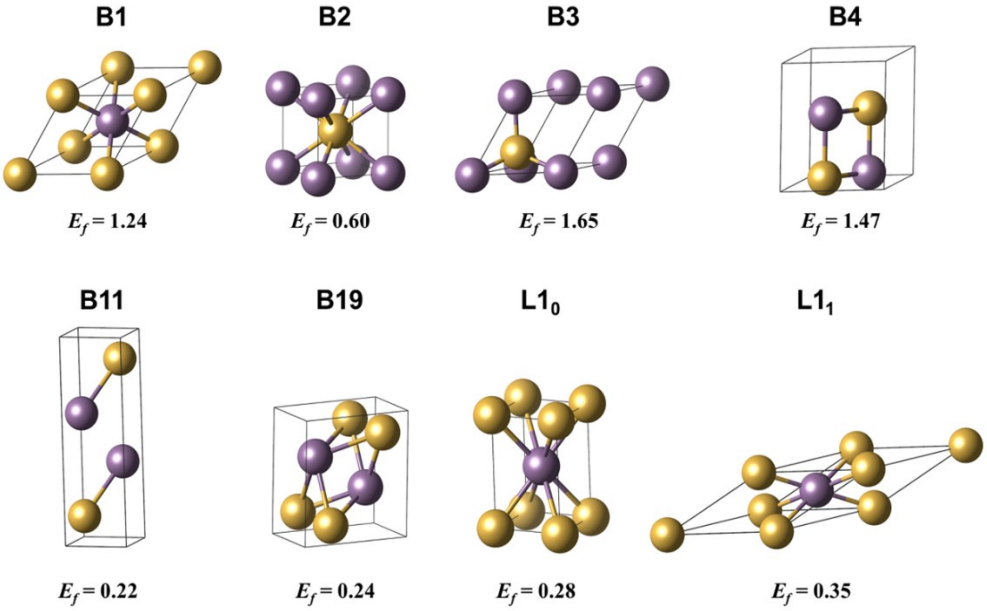

Fig. S5 (a) Molecular orbital electron configurations of Mo–Mo, Mo–Au, and Au–Au. The type of bonding (σ, π, δ, nb) is characterized by the number of nodes parallel to the bond, and the bonding characteristics (bonding denoted with a single character without *; anti-bonding denoted with superscript *; non-bonding denoted as nb) is classified by the phase interaction between two atomic orbitals. Based on the summation of bonding and anti-bonding, the bond character is shown as Mo–Mo: sextuple, Au–Au: single, and Mo–Au: 0.5 bonds, very weak binding), where the

molecular orbitals are calculated at the UPBE/def2-TZVP levels of theory. The Mo–Au has a total of 17 electrons ($11e^-$ from Au & $6e^-$ from Mo), which comprise 17 molecular orbitals in the unrestricted calculation. *S* represents the multiplicity of the ground state for each dimer. The Mo-Au bond length showing the Wiberg bond index of 1.04 is longer than Au-Au, and Mo-Mo bond lengths, reflecting weak immiscibility between Mo and Au atoms, in agreement with the qualitative analysis of bond orbitals. (b) Formation energy (eV) per atom and unit cell structure for binary metal alloys (AB) of all eight possible phases. The formation energy per atom (E_f in eV/atom) calculated by $E_f = (E(A_nB_m) - n\mu_{Mo} - m\mu_{Au})/(n+m)$, where $E(A_nB_m)$, n, m, $\mu_{Mo,}$ and μ_{Au} is the total energy of alloy, number of Mo atoms in unit cell, number of Au atoms in unit cell, the chemical potential of Mo, and chemical potential of Au, respectively. The positive E_f means immiscible alloys (Au: yellow; Mo: purple), showing that Mo-Au are immiscible, which results in Mo atoms embedded at Au surface.

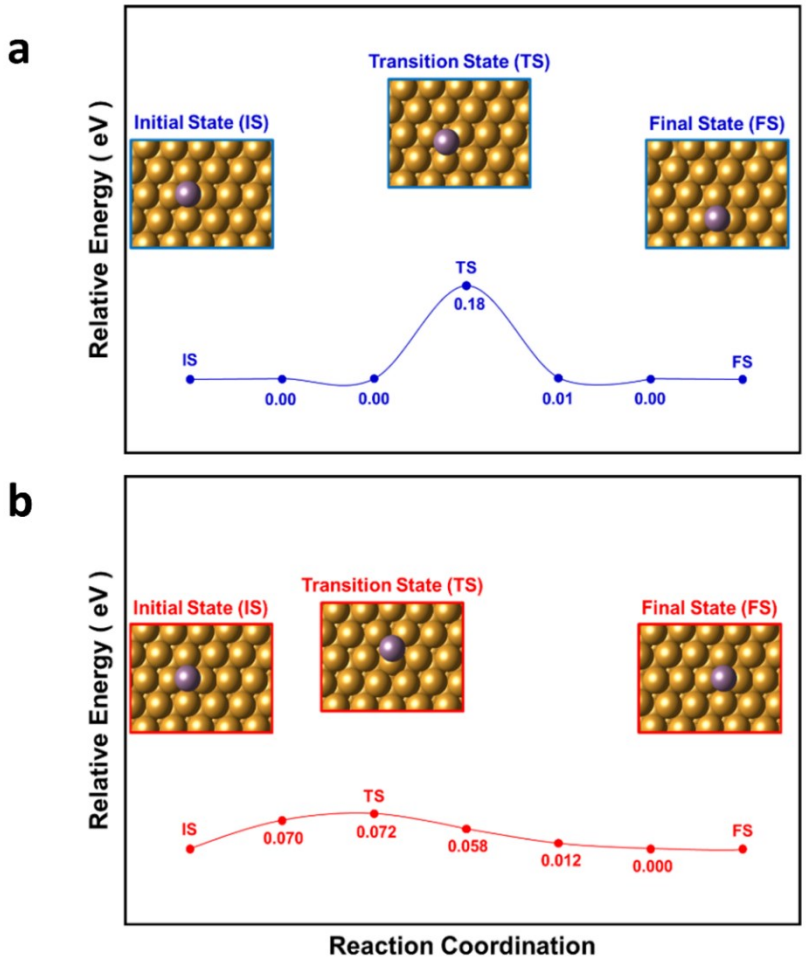

Fig. S6 Diffusion of Mo on/into Au surface. DFT-predicted diffusion path of a Mo adatom on Au(111) surface and its reaction barrier. (a) Diffusion in the vertical y-direction (the barrier: 0.18 eV). (b) Diffusion in the horizontal x-direction (0.072 eV). The most stable bridge site and adjacent bridge site are selected as initial state and final state,

respectively (Mo: purple; Au: yellow). For each diffusion case, the transition state is calculated as a tilted hollow site on Au(111) surface. Since the diffusion barrier of a Mo atom on the Au(111) surface is only 0.072 eV, the diffusion is very fast even at RT (0.025 eV). The replacement of a Mo atom into the Au surface is possible only when the Au surface has vacant sites since the atomic diameter size of Mo is only slightly smaller than that of an Au atom (by 0.3 Å as compared with the diameter of 3.3 Å for an Au atom). One Mo atom can occupy a mono-vacant site for Au, while two Mo atoms, a di-vacant site. The heat of formation energies of a mono-vacant and di-vacant sites of Au are 0.94 eV and 1.56 eV, respectively.[7,8] Thus, it is mostly expected that a single Mo atom of Mo atoms/clusters can occupy one of mono-vacant sites of Au surface.

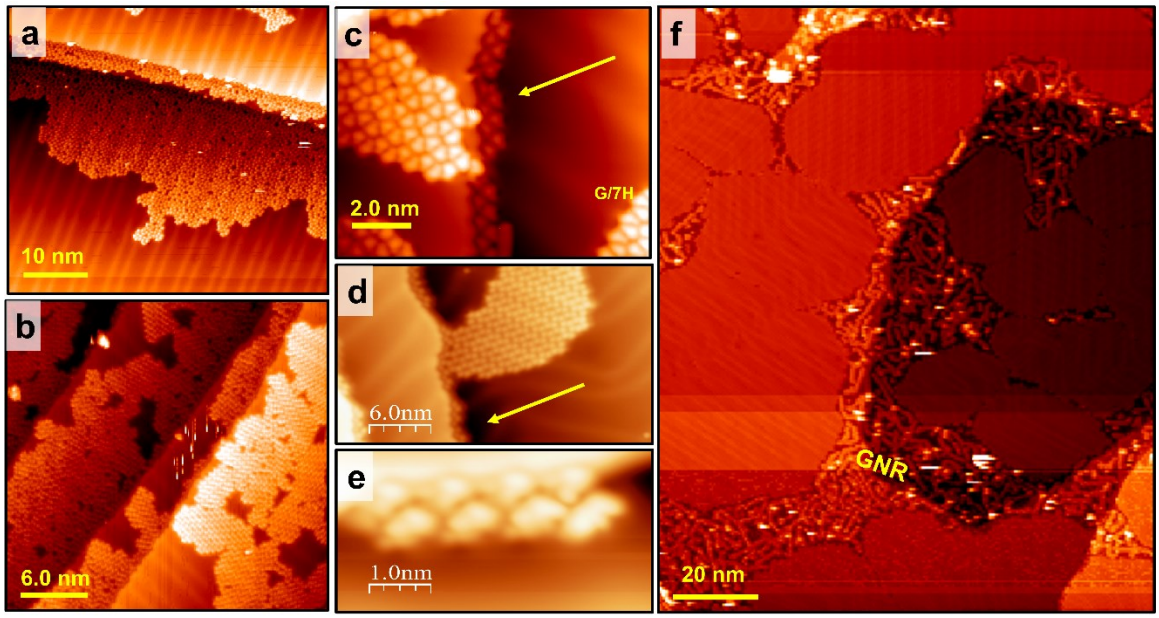

Fig. S7 Chemical bonding of G/9H and G/7H molecules with the surface, within the terrace, or at step edges. (a) The growth of the surface assemblies of guanine molecules on the Mo-doped Au surface begins from step edges. It is independent of the surface terrace width. Due to reconstructed patterns and low-coordinated Au atoms, step edges represent preferential nucleation sites for supramolecular structures' growth. Implanted Mo atoms at Au surface are also adsorption zones, but in case of doping densely, overdoped Au surface makes adsorbed guanine molecules rather fixed with a lack of conformality to GQ lattice due to relatively strong covalent bonds with the surface. Therefore, the rest of the guanine molecules have no choice other than to make HBs with an array of initial molecules that are not compatible with the GQ network's geometry. It is worth mentioning that surface step edges are still preferential nucleation sites even in the case of the overdoped surface. Au(111) surface is overdoped with Mo atoms by less annealing duration (830 K for 5 min), a few separated porous structures are appeared, but GQ network formation is unlikely due to extra anchored molecules. (b) at 400 K G/9H molecules on over-doped Mo-Au(111) surface partially transformed to the close-packed structure. (c) The disordered phase on densely Mo-doped

Au surface is fully transformed to G/7H after it annealed at 460 K. Scanning conditions for (a-c): I_t = 0.02 nA, V_s = +0.9 V. (d) STM image of the G/7H close-packed structure on pristine Au(111) surface after annealing at 400 K. The whole structure rearranged, except guanine molecules bonded at step edges. In contrast with the GQ network, the close-packed lattice has the flexibility to adapt with guanine molecules bonded at step edges or Mo atoms. Scanning conditions: I_t = 0.02 nA, V_s = -0.9 V. (e) Two arrays of guanine molecules adsorbed at pristine Au step edges are covalently bonded with Au atoms after it is annealed at 400 K. The geometry of the step edges determines the orientation of the initial seed. (f) At 520 K, GQ networks on Mo-doped Au surface with GNR pre-synthesis fully transformed into the large islands of the close-packed structure. GNRs were relocated while stayed separated from guanine SAs and gathered around step edges. Scanning conditions: I_t = 0.02 nA, V_s = -0.9 V. Scale bar: 10 nm in panel a, 6.0 nm in panel b, 2.0 nm in panel c, 6.0 nm in panel d, and 1.0 nm in panel e, and 20 nm in panel f.

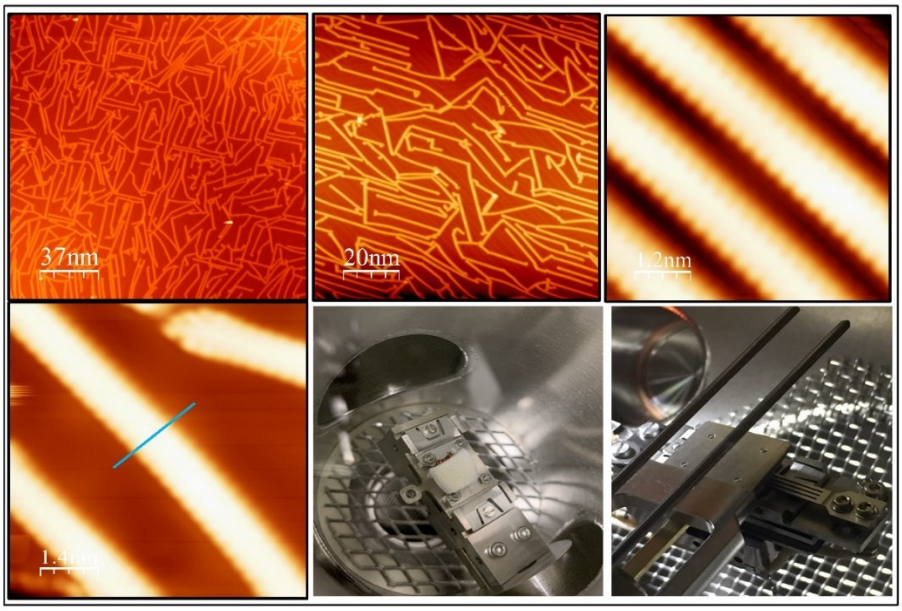

Fig. S8 Bare 7-AGNRs on Au(111) surface. STM measurements show based on the height and width of 7-AGNR, synthesis of 7-AGNR from DBBA precursor was successful.[9–12] DCT method gives the opportunity of having various concentrations of GNR on Au(111) surface in one sample. Scanning conditions: I_t = 0.1 nA, V_s = +0.75 V. The DBBA stamp was made by installing a cotton ball on the sample plate.[10] A small portion of the tip head of the stamp was gently pressed into a container of monomers in the air. The coated stamp was placed into the UHV for a long time and then touched quite gently against only a corner of the substrate by micro placer; therefore, various concentrations of GNRs on the surface were formed (the more distant from the corner, the less concentrated on the surface).

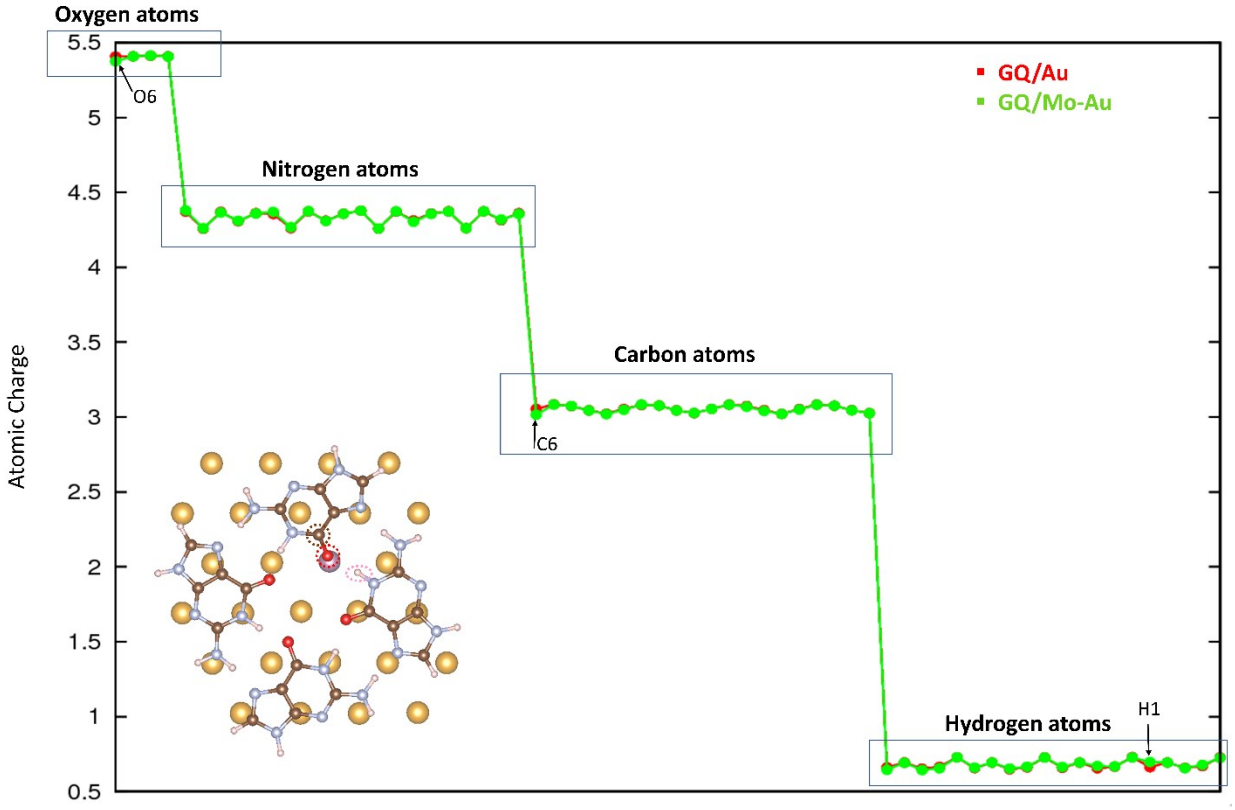

Fig. S9 The DFT calculated muffin-tin charges and intraquartet hydrogen bond length for GQ network adsorbed on pristine Au(111) surface (red), and GQ network adsorbed on Mo-doped Au(111) surface (green). The muffin-tin charges mainly decrease for O6 and increase for hydrogen associated with hydrogen bond with O6, which is caused by the covalent bond between Mo and O6. In addition, it results in vertical movement of O6 atom toward the Mo atom, where O6-H hydrogen bond length increases from 1.65 Å to 2.0 Å as shown in the inset image. Thus the suppressed effective charges and elongated bond length associated with O6-H weakens the hydrogen bond strength.

REFERENCES

1 Y. Cho, S. K. Min, J. Yun, W. Y. Kim, A. Tkatchenko and K. S. Kim, *J. Chem. Theory Comput.*, 2013, **9**, 2090–2096.

2 S. K. Min, W. Y. Kim, Y. Cho and K. S. Kim, *Nat. Nanotechnol.*, 2011, **6**, 162–165.

3 A. C. Rajan, M. R. Rezapour, J. Yun, Y. Cho, W. J. Cho, S. K. Min, G. Lee and K. S. Kim, *ACS Nano*, 2014, **8**, 1827–1833.

4 M. M. Biener, J. Biener, R. Schalek and C. M. Friend, *Surf. Sci.*, 2005, **594**, 221–230.

5 X. L. Li, G. Ouyang and G. W. Yang, *Nanotechnology*, 2008, **19**, 505303.

6 T. B. Massalski, H. Okamoto and L. Brewer, *Bull. Alloy Phase Diagrams*, 1986, **7**, 449–452.

7 S. Notes and M. L. Wasz, 1992, **71**, 71–76.

8 T. Hehenkamp, *J. Phys. Chem. Solids*, 1994, **55**, 907–915.

9 J. Cai, P. Ruffieux, R. Jaafar, M. Bieri, T. Braun, S. Blankenburg, M. Muoth, A. P. Seitsonen, M. Saleh, X. Feng, K. Müllen and R. Fasel, *Nature*, 2010, **466**, 470–473.

10 J. D. Teeter, P. S. Costa, P. Zahl, T. H. Vo, M. Shekhirev, W. Xu, X. C. Zeng, A. Enders and A. Sinitskii, *Nanoscale*, 2017, **9**, 18835–18844.

11 P. Ruffieux, J. Cai, N. C. Plumb, L. Patthey, D. Prezzi, A. Ferretti, E. Molinari, X. Feng, K. Müllen, C. A. Pignedoli and R. Fasel, *ACS Nano*, 2012, **6**, 6930–6935.

12 L. Talirz, P. Ruffieux and R. Fasel, *Adv. Mater.*, 2016, **28**, 6222–6231.